Defect-free Naphthalene Diimide Bithiophene Copolymers with Controlled Molar Mass and High Performance via Direct Arylation Polycondensation

Rukiya Matsidik,[†,‡] Hartmut Komber,[*,§] Alessandro Luzio,[‖] Mario Caironi,[‖] and Michael Sommer[*,†,‡]

[†]Makromolekulare Chemie, Universität Freiburg, Stefan-Meier-Straße 31, 79104 Freiburg, Germany
[‡]Freiburger Materialforschungszentrum, Stefan-Meier-Straße 21, Universität Freiburg, 79104 Freiburg, Germany
[§]Leibniz Institut für Polymerforschung Dresden e.V., Hohe Straße 6, 01069 Dresden, Germany
[‖]Center for Nanoscience and Technology @PoliMi, Instituto Italiano di Tecnologia, Via Pascoli 70/3, 20133 Milano, Italy

Ⓢ Supporting Information

ABSTRACT: A highly efficient, simple, and environmentally friendly protocol for the synthesis of an alternating naphthalene diimide bithiophene copolymer (PNDIT2) via direct arylation polycondensation (DAP) is presented. High molecular weight (MW) PNDIT2 can be obtained in quantitative yield using aromatic solvents. Most critical is the suppression of two major termination reactions of NDIBr end groups: nucleophilic substitution and solvent end-capping by aromatic solvents via C−H activation. In situ solvent end-capping can be used to control MW by varying monomer concentration, whereby end-capping is efficient and MW is low for low concentration and vice versa. Reducing C−H reactivity of the solvent at optimized conditions further increases MW. Chain perfection of PNDIT2 is demonstrated in detail by NMR spectroscopy, which reveals PNDIT2 chains to be fully linear and alternating. This is further confirmed by investigating the optical and thermal properties as a function of MW, which saturate at $M_n \approx 20$ kDa, in agreement with controls made by Stille coupling. Field-effect transistor (FET) electron mobilities μ_{sat} up to 3 cm^2/(V·s) are measured using off-center spin-coating, with FET devices made from DAP PNDIT2 exhibiting better reproducibility compared to Stille controls.
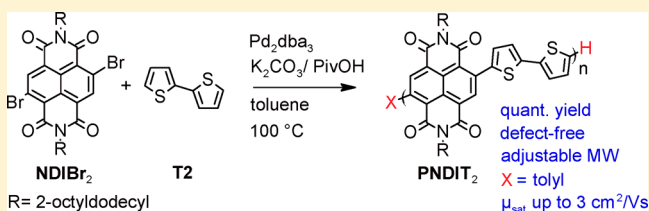
1. INTRODUCTION

High-performance conjugated copolymers exhibiting efficient electron transport are critical components in complementary circuits, polymer photovoltaics, and organic thermoelectrics.[1−3] Among the few chemical structures with suitable n-channel properties available, poly{[N,N′-bis(2-octyldodecyl)-naphthalene-1,4,5,8-bis(dicarboximide)-2,6-diyl]-alt-5,5′-(2,2′-bithiophene)}, here abbreviated as PNDIT2, is an impressive exception with high electron mobilities, low energetic disorder, and unconventional morphological behavior.[4−7] However, although many derivatives of PNDIT2 have since been made,[8] only isolated examples have shown slightly enhanced optoelectronic performance compared to the benchmark material PNDIT2,[9,10] which thus retains its leading position. Notably, the most unfavorable issue with PNDIT2 or other naphthalene diimide (NDI) main-chain copolymers is related to their preparation by mostly Stille polycondensation involving highly neurotoxic organo-stannanes.[11] Recently, Senkovskyy et al. disclosed a new synthesis of PNDIT2 based on the polymerization of radical anions, which has meanwhile been optimized to proceed at room temperature within minutes and with very small loadings of palladium.[12,13] However, this method cannot be applied without restriction as only a few chemical structures are accessible due to the symmetric structure of the monomer. Moreover, the preparation and

reproducibility of the Rieke zinc suspension is tedious and renders this protocol a challenge.

The most simple and straightforward way to construct conjugated polymers is the direct activation of a C−H bond. In direct arylation polycondensation (DAP), the synthesis of monomers with organo-metallic functional groups is redundant, which makes this method in principle superior compared to classical transition-metal-catalyzed polycondensation.[14−17] As a result, syntheses by DAP are faster and less expensive, require less resources, produce less waste, and hence make a substantial contribution to the development of sustainable chemistries. Moreover, toxicity issues related to Stille couplings can elegantly be circumvented. It is important to realize that while impressive progress has been made in the synthesis of p-type polymers via DAP during the last years,[18−23] the synthesis of high-molar-mass n-type copolymers, especially NDI copolymers, was either unsuccessful,[24] suffered from solubility issues and hence led to oligomers only,[10] or resulted in moderate electron mobilities.[25]

Here we report an efficient and surprisingly simple protocol toward the quantitative synthesis of PNDIT2 with high and controllable molecular weight (MW) via the DAP of

Table 1. Summary of Reaction Conditions of PNDIT2[a]

entry	solv	Pd$_2$dba$_3$ (%)	phosphine	T (°C)	conc (M)[b]	time (h)[c]	M_n/M_w (kDa)[d]	yield (%)[e]
1	Tol	1	–	70	0.05	72	9.3/13	65
2	Tol	1	–	80	0.05	72	8.6/12	73
3	Tol	5	–	80	0.05	72	7.6/11	70
4	Tol	0.5	–	80	0.05	72	–	–
5	Tol	1	–	80	0.05	144	8/11	77
6	THF	5	–	80	0.05	72	4/6	24
7	THF	2	HP(Bu)$_3$BF$_4$	80	0.05	72	–	–
8	Tol	1	–	90	0.05	72	7.9/10	68
9	Tol	1	–	100	0.05	72	9.3/13	66
10	Tol	1	–	70	0.1	72	10/13	67
11	Tol	1	–	80	0.1	72	10.2/14	69
12	Tol	1	–	90	0.1	72	10.4/14	69
13	Tol	1	–	100	0.1	72	11.6/16	70
14	Tol	1	–	100	0.2	30	21/45	98
15	Tol	1	–	100	0.3	14	26/64	99
16	Tol	1	–	100	0.4	14	28/78	99
17	Tol	1	–	80	0.5	14	17/36	96
18	Tol	1	–	90	0.5	14	31/91	99
19	Tol	1	–	100	0.5	14	35/124	100
20	Tol	1	–	100	0.6	6	22/47	99
21	Tol	1	–	110	0.5	2	24/73	99
22	Tol	0.5	–	100	0.5	5	17/38	98
23	Tol	0.1	–	100	0.5	20	17/32	95
24	CB	1	–	100	0.5	2	41/162	99
25	CB	0.1	–	100	0.5	20	20/42	97
26	Tol	1	PCy$_3$	100	0.5	72	–	–
27	Tol	1	PPh$_3$	100	0.5	72	–	–
28	Tol	1	P(o-anisyl)$_3$	100	0.5	72	7/8	45
29	Tol	1	HP(^{t}Bu$_2$Me)BF$_4$	100	0.5	72	4/5	2

[a]PivOH (1 equiv) and K$_2$CO$_3$ (3 equiv) were used in all entries. Tol, THF, and CB are toluene, tetrahydrofuran, and chlorobenzene, respectively. [b]Concentration of NDIBr$_2$ in the aromatic solvent. [c]Reduced reaction time in case the mixture solidified. [d]From SEC in CHCl$_3$. [e]Isolated yield after Soxhlet extraction with isohexane.

unsubstituted bithiophene (T2) with NDIBr$_2$. Using tris-(dibenzylideneacetone)dipalladium (Pd$_2$dba$_3$) as catalyst, K$_2$CO$_3$, and PivOH, PNDIT2 free of any main-chain defect arising from either homocoupling or unselective C–H activation,[26–29] can be synthesized in aromatic solvents with low catalyst loadings and in short times. The materials obtained under reduced costs (PNDIT2 made by DAP is estimated to be cheaper by ~35% compared to standard procedures[30,31]) show optical, thermal, and electronic properties that are at least identical to controls made by Stille polycondensation and exhibit organic field-effect transistor (OFET) electron mobilities of up to 3 cm^2/(V·s). All entries of PNDIT2 made via DAP are compiled in Table 1.

2. RESULTS AND DISCUSSION

Recently, we realized that nucleophilic substitution of the monomer NDIBr$_2$ under direct arylation (DA) conditions with an excess of pristine thiophene was greatly suppressed in nonpolar solvents such as toluene.[32] Obviously, this poses ideal conditions under which polycondensation can be conducted efficiently, and thus we investigated the stoichiometric reaction between NDIBr$_2$ and T2 and the resulting products PNDIT2 in detail (Scheme 1).

Under phosphine-free conditions with Pd$_2$dba$_3$, K$_2$CO$_3$, and PivOH at relatively low monomer concentrations between 0.05 and 0.1 M in toluene (these concentrations are 2–4 times larger than typical concentrations for Stille polycondensation),

Scheme 1. Synthesis of PNDIT2 via Direct Arylation Polycondensation
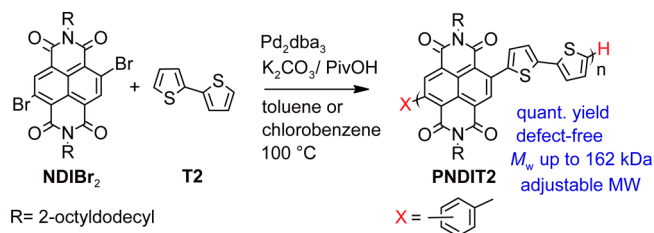
oligomeric materials were obtained in moderate yield. Increasing the reaction temperature from 70 to 100 °C or changing the solvent from toluene to THF did not improve MW considerably (Table 1, Figure 1a). Most strikingly, increasing monomer concentration up to 0.6 M turned out to be most effective to increase and control MW. The best results were obtained for 0.5 M monomer concentration in toluene at 100 °C, for which a maximum $M_{n,SEC}$ = 35 kDa was obtained (Figure 1a, Table 1, entry 19). For comparison with literature data, the M_w values are given as well, which show the same trend with increasing monomer concentration. Values for M_w are nominally high, but especially affected by aggregation so that these values may not be reliable. For this reason the dispersities Đ are likely to be overestimated as well. Importantly, typical M_n values for PNDIT2 samples made by Stille polycondensation exhibit values similar to the best results
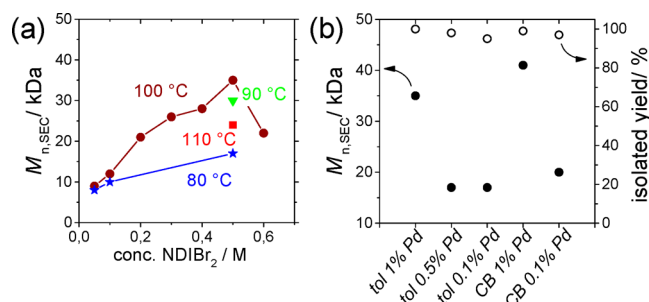
Figure 1. (a) Evolution of M_n of PNDIT2 with monomer concentration in toluene as solvent. (b) M_n and isolated yields in toluene (tol) or chlorobenzene (CB) for different amounts of Pd$_2$dba$_3$.

in Table 1, entry 19, made in toluene. Reaction temperatures that were both higher and lower than 100 °C resulted in decreased MWs. Also lower and higher concentrations than 0.5 M both gave lower MWs. To our contentment, the isolated yields of soluble product after Soxhlet extraction with isohexane were quantitative for the higher temperatures and concentrations (Figure 1b). Below it will be shown that the reason for the good MW control with increasing concentration originates from a drastically accelerated polycondensation reaction that is much faster than end-capping of NDIBr chain ends via C−H activation of toluene.

These results are indicative for a very efficient DAP. It is interesting to note that the herein used catalytic system without a phosphine ligand is very efficient but fails for the DA of an excess of thiophene and 3,7-dibromobenzothiadiazole, where Pd black precipitates.[32] To further test the catalytic efficacy and the robustness of the system, we performed the reaction at lower Pd loadings. For amounts of Pd$_2$dba$_3$ down to 0.1 mol %, the quantitative yield was maintained albeit M_n was lower (Figure 1b, Table 1, entries 22 and 23). Performing DAP at high monomer concentration requires good solubility of the conjugated polymer to avoid gelation of the reaction mixture at early times. While toluene is a good solvent for PNDIT2, chlorinated aromatic ones are better.[33] Using chlorobenzene (CB), an even higher $M_{n,SEC}$ = 41 kDa was obtained under identical reaction conditions, which can be attributed to the increased solubility of PNDIT2 in CB (Table 1, entry 24). Favorably, the decreased C−H reactivity of CB compared to toluene additionally enabled higher MWs by decreasing the probability for in situ end-capping, as will be explained below. Decreasing the amount of Pd$_2$dba$_3$ from 1% to 0.1% again led to quantitative yields and similarly decreased molar masses, but the overall numbers were always higher for CB than for toluene (Figure 1b, Table 1, entry 25). Also with CB as the solvent the highest MW was obtained for 0.5 M and 100 °C. Somewhat surprisingly, adding various phosphines to the best conditions shown in entry 19, only oligomeric material was obtained (Table 1, entries 26−29).

To understand why such monumental differences in molar mass were observed as a function of the monomer concentration, the solvent, and the presence of a phosphine, ^{1}H NMR spectroscopy was performed with a particular focus on end group analysis to characterize polymer chain ends and thus the type of termination reaction (Figure 2).

A major effort was made to unambiguously assign all end groups by using a variety of model compounds and two-dimensional spectra, and by estimating chemical shift increments of unsymmetrically substituted NDI and T2 units (see
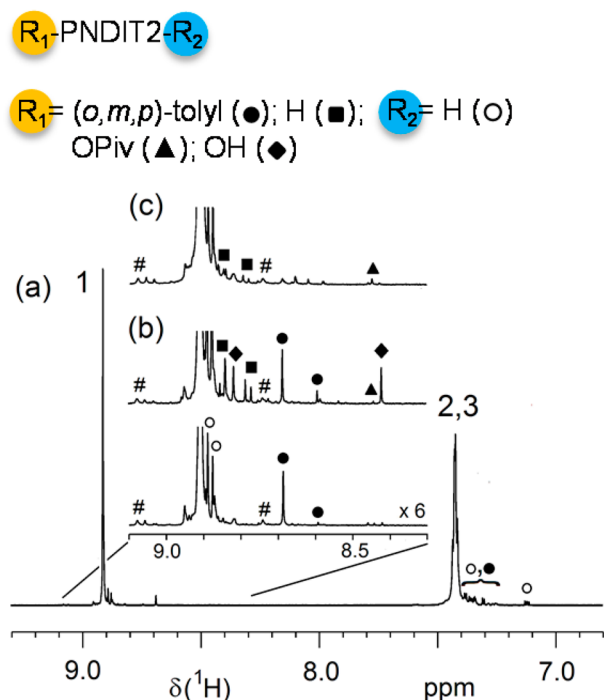

Figure 2. ^{1}H NMR analysis of PNDIT2. (a) Aromatic region of PNDIT2 made in toluene at 0.5 M with backbone signals of NDI (1) and T2 (2,3) and enlarged region of NDI end group (EG) signals (for full spectrum see Figure SI-10 in Supporting Information). (b) PNDIT2 made in toluene at 0.05 M. (c) Enlarged region of a high-molar-mass sample prepared in CB (for full spectrum see Figure SI-11 in Supporting Information). The intensity of the backbone signal is the same for all enlarged regions (a)−(c). Spectra were taken in C$_2$D$_2$Cl$_4$ at 120 °C; # marks ^{13}C satellites.

Supporting Information for details, compounds, and spectra, Figures SI-1−SI-9, Table SI-1). Most conveniently, it turned out that almost any side reaction of NDIBr chain ends gave rise to additional, isolated singlets in the ^{1}H NMR spectra, which greatly facilitated analysis. Depending on the reaction conditions, a varying number of signals with low intensity next to the backbone signals was observed. Figure 2a displays the aromatic region of the ^{1}H NMR spectrum of PNDIT2 from Table 1, entry 19, with a high M_n = 35 kDa and with all end groups assigned (see Figure SI-10 in the Supporting Information). Using model reactions of monobrominated NDIBr with the solvent only, end groups were assigned, and CB was found to be much less reactive than toluene with respect to C−H activation. Strikingly, under optimized conditions, i.e., high concentration, 100 °C, and with aromatic solvents, only tolyl-terminated NDI (o:m:p ≈ 5:40:55) and H-terminated T2 chain ends were found. Thus, we conclude that the reaction system is absolutely stable with no observable end group degradation such as dehalogenation or homocoupling.[26] The only side reaction that takes place under these conditions is the in situ termination of NDIBr chain ends by C−H activation of the aromatic solvent, which can to a large extend be adjusted by monomer concentration. As the overall rate of polycondensation is proportional to [NDIBr$_2$]^2 while the rate of end-capping is proportional to [NDIBr$_2$][tol], an increasing monomer concentration increases the ratio of the rate of step growth to the rate of end-capping, and thus leads to higher molar mass. Moreover, the presence of tolyl end groups but the absence of chlorophenyl end groups of PNDIT2 made by DAP

in toluene and CB, respectively, points to different reactivities toward C−H activation, which poses an additional mean to control molar mass.

With this knowledge in mind, we investigate the origins of the drastically reduced molar masses of PNDIT2 made in THF and in the presence of an additional phosphine. Previously, we observed that NDIBr$_2$ is prone to nucleophilic substitution in DMAc leading to hydroxylation.[32] Oligomeric PNDIT2 made by DAP in THF exhibited a major fraction of hydroxylated NDI chain ends, confirming that nucleophilic substitution did also play a detrimental role here (Table 1, entry 6; see Figures SI-6 and SI-12 in Supporting Information). In addition to OH end groups, we also observed two new singlets arising from pivaloate terminated NDI chains (confirmation with NDI-pivaloate model compound, see Figure SI-5 in Supporting Information). This side reaction either arises from a nucleophilic aromatic substitution reaction, or from a catalytic intermediate involving a palladium species from which a possible intramolecular attack of pivaloate to the NDI chain end is possible. The latter scenario is also supported by the fact that an increasing concentration of Pd$_2$dba$_3$ led to increasing pivaloate termination in model reactions. However, as nucleophilic substitution of NDIBr is also possible in the absence of a Pd catalyst, both mechanisms with and without Pd appear possible. Entries in which a phosphine was used in addition to Pd$_2$dba$_3$ gave mainly hydroxyl-terminated NDI chains, presumably via a similar process involving palladium (Table 1, entry 28; see Figure SI-13 in Supporting Information). Pivaloate chain ends were also observed in toluene without phosphine at low monomer concentration, albeit with much lower intensity (Table 1, entry 9; see Figure SI-14 in Supporting Information). Thus, it is concluded that nucleophilic substitution of NDIBr chain ends is most efficient in polar solvents. Importantly, this side reaction occurs for low concentration in toluene as well but with decreased intensity and is almost fully suppressed at high concentrations. Pivaloate-terminated NDI chains potentially act as precursors for HO-terminated chains as a result of subsequent saponification (Scheme 2).

Having identified solvent end-capping and nucleophilic substitution, which have not yet been discussed as side reactions of DAP (the usually observed dehalogenation reaction did only play a very minor role here), and having optimized the conditions under which these processes can be suppressed and controlled, we turned our attention to possible side reactions
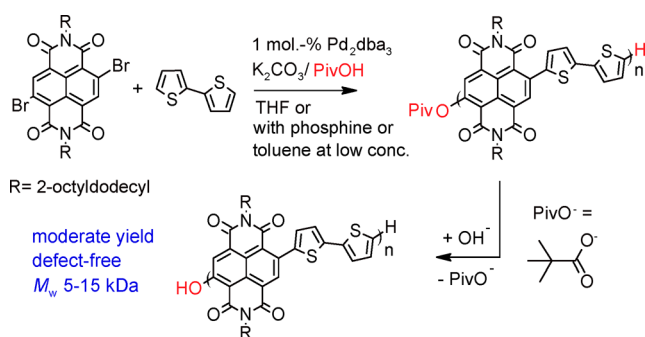
such as homocouplings or unselective C−H arylation, both of which cause electronic main chain defects in conjugated polymers prepared by DAP.[26−29,34] Obviously, as all low-intensity signals of the ^{1}H NMR spectrum were successfully assigned, the presence of main chain defects can be excluded indirectly as those are expected to give chemical shifts significantly different from backbone and end group signals. However, a direct proof of the absence of homocouplings is additionally given by a low-MW model compound T2-NDI-NDI-T2 and by the copolymer PNDIT4, which mimic the chemical shifts of such species. Characteristic chemical shifts of these homocouplings are not found in the ^{1}H NMR spectra of all PNDIT2 samples made in this study, which unambiguously demonstrate the absence of such species (see Figures SI-8 and SI-9 and Table SI-1 in Supporting Information). The absence of unselective C−H activation of T2 (also referred to as "β-arylation") leading to kinked backbones with presumably devastating electronic properties is assumed from the fact that all additional signals with low intensity are assigned after end group analysis.

With a consistent series of defect-free PNDIT2 samples with increasing molar mass and mostly identical end groups in hand, the optical, thermal, and electronic properties of PNDIT2 for $M_{n,SEC} = 10−40$ kDa were investigated and compared to those of controls made by conventional Stille coupling. Figure 3
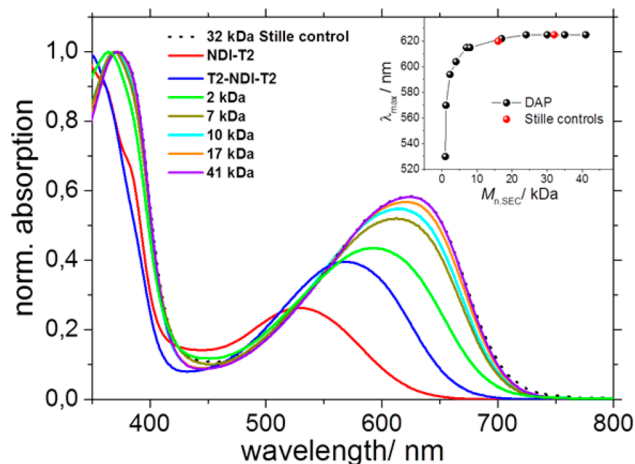

Figure 3. UV−vis spectroscopy of PNDIT2 made by DAP as a function of M_n in 2-chloronaphthalene. The inset shows the dependence of λ_{max} of the low-energy band with M_n.

shows the absorption spectra in 2-chloronaphthalene as a solvent in which PNDIT2 chains are not aggregated.[33] The many defect-free samples with different degrees of polymerization allow to obtain information about the conjugation length in solution. For comparison, the well-defined oligomers NDI-T2 and T2-NDI-T2 are shown. Both intensity and maximum wavelength of the low-energy band (λ_{max}) increase with increasing molar mass, whereby λ_{max} saturates for $M_n = 20$ kDa at 625 nm, which is in good agreement with values of high-molar-mass materials.[33] Further, the absorption spectra of higher molar mass PNDIT2 DAP samples match very well with that of a reference sample made by Stille polycondensation ($M_n = 32$ kDa, $M_w = 172$ kDa). Values of λ_{max} from Stille controls with lower molar mass fitted well into that plot (see inset in Figure 3). This corroborates the results from NMR in that the presented synthesis of PNDIT2 by DAP provides truly

Scheme 2. Nucleophilic Substitution of NDIBr Chain Ends as Origin of Reduced Molar Mass of PNDIT2 in THF, at Low Monomer Concentration in Toluene, or in the Presence of a Phosphine

alternating chains where the wavelength of the low-energy band is determined only by the length of the chain, and not by kinks or other defects in the polymer main chain which would severely limit conjugation length.

To additionally corroborate the defect-free nature of PNDIT2 made by DAP, the thermal properties were investigated as a function of MW (see Figures SI-15−SI-17 and Table S-2). The melting points T_m and melting enthalpies ΔH_m obtained from differential scanning calorimetry (DSC) increased with molar mass up to a saturation regime of T_m = 310 °C and ΔH_m = 9.2 J/g, respectively, which is again in line with data from high-molar-mass samples made by Stille coupling. It is clear that already one single kink or homocoupling defect would substantially lower both these values as the crystallizable segment length would be strongly reduced.[35] Thus, also the thermal data confirms the NMR data with respect to the defect- and kink-free nature of PNDIT2 chains made via DAP. What remains open at this point is why the Stille controls with low molar mass exhibit melting enthalpies that are reduced by a factor of almost 2 for comparable MWs (see Table SI-2). For semicrystalline polymers dispersity is known to influence the degree of crystallinity.[35] Additionally, fractionated crystallization can occur which complicates the extraction of melting enthalpies for low-molar-mass materials.[36] However, the dispersities for both DAP and Stille controls were very similar (see Table SI-2), and a correlation with melting enthalpies does not seem to be the case. Next to these factors, sample purity and end groups are further potential parameters that need to be considered in due course.

To assess and compare the electronic performance of PNDIT2 made via the newly established DAP protocol, we fabricated and characterized bottom contact, top-gate field-effect transistors (FETs) using a directional deposition method for the semiconductor to optimize the charge transport.[37] The transfer characteristics were measured in the saturation regime (V_{DS} = 60 V) and field effect mobility values (μ) were extracted according to the gradual channel approximation (Figure 4).[38] For all samples ideal n-channel field effect behavior was found as evidenced by the typical transfer curve in the electron accumulation regime reported in Figure 4a (where the current measured at negative V_G values reflects the p-channel mobility, typically poor, still present in PNDIT2 films).[39]

Saturation mobilities (μ_{sat}) show an evident V_G dependence, as reported in Figure 4b, in agreement with recent literature on some of the best performing n-type polymeric semiconductors and likely owing to an effect of the lateral field on injection and/or transport.[40−45] In Figure 4c, the μ_{sat} values at $V_G = V_{DS}$ = 60 V for PNDIT2 made by DAP are shown and compared to controls made via Stille polycondensation. Only a slight dependence on M_n was found, with all values being on the order of 1 cm^2/(V·s) and displaying a maximum around M_n = 32 kDa, independently on the synthetic procedure employed. Interestingly, almost identical performance can be observed for the best DAP ($\mu_{sat,mean}/\mu_{sat,max}$ = 2.6/2.9 cm^2/(V·s)) and Stille batches ($\mu_{sat,mean}/\mu_{sat,max}$ = 2.5/3.2 cm^2/(V·s)), which are the best performances recorded for PNDIT2,[40] and which are generally among the highest mobilities of solution processed n-channel semiconductors reported so far.[46,47] For a typical output curve and details on FETs fabricated by standard spin coating, see Figures SI-18 and SI-19, respectively. On the one hand, this is strong evidence supporting high batch purity and the defect-free nature of PNDIT2 made by DAP; on the other
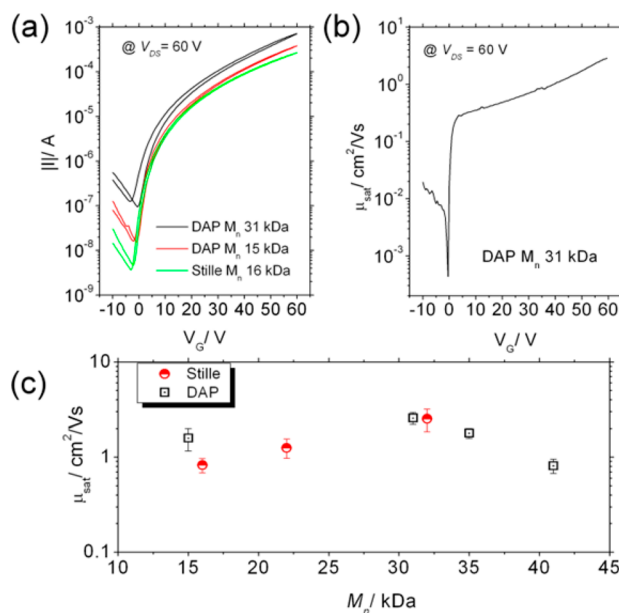

Figure 4. Typical transfer characteristics (a) and saturation mobility vs V_G plot (b) of DAP-synthesized PNDIT2-based FETs. (c) Average saturation mobilities extracted at $V_{DS} = V_G$ = 60 V vs M_n (error bars are from standard deviations for averages of 10 devices for each molecular weight).

hand it indicates the effectiveness of solution pre-aggregation process in both cases, a key aspect to achieve the best transport properties in PNDIT2 films.[43] To corroborate this aspect, the UV−vis spectra of toluene solutions from which active films of FETs were deposited are shown in Figure SI-20, in which optical markers of aggregation are clearly visible and comparable.[33] It is noteworthy that for lower M_n values (~15 kDa) a diversification of mobility values was found, whereby PNDIT2 made by DAP samples displayed superior performance than Stille controls ($\mu_{sat,DAP}/\mu_{sat,Stille}$ = 1.58/0.82 cm^2/(V·s)). Also the pre-aggregation process seemed to be less prevalent for the Stille controls at this MW region (Figure SI-20), likely leading to inferior interconnectivity within the film microstructure and lower mobilities as a consequence. This picture is further confirmed by the DSC characterization reported in Table SI-2, where both the melting points (T_m) and the enthalpies of fusion (ΔH_m) are higher for DAP samples at M_n = 16 kDa ($T_{m,DAP}/T_{m,Stille}$ = 300.3/287.4 °C, $\Delta H_{m,DAP}/\Delta H_{m,Stille}$ = 4.39/2.14 J/g), reflecting an enhanced degree of crystallinity of films made from DAP samples. While this difference in ΔH_m is only one possible explanation for the enhanced transport properties of low-molar-mass DAP samples, the precise effect of varying degrees of crystallinity on OFET charge transport where the top layer is probed is still an open question. Potentially higher purities of DAP batches due to the inherent absence of tin residues could be another possibility, which is a subject of ongoing investigations.[48,49]

3. CONCLUSION

We have demonstrated an efficient synthetic protocol suitable for the preparation of PNDIT2 with high and controllable molar mass via direct arylation polycondensation in quantitative yield. The obtained materials are defect-free in nature as demonstrated by detailed NMR studies, which is corroborated by the optical and thermal properties of a large number of PNDIT2 samples with different molar masses together with

controls. This is the first example of the benchmark material PNDIT2 made by DAP. High electron mobilities up to 3 cm^2/(V·s) are obtained using off-center spin-coating, which are at least equal to those of analogues made by conventional cross-coupling. Estimations regarding cost savings of the presented synthesis route compared to classical Stille polycondensation are about 35%, which is a highly promising value given the increased atom-economy and the concomitant reduced and much less toxic waste of the DAP route. Together with the intriguing possibility to control molar mass and end groups via in situ toluene end-capping, the presented protocol is superior in all practical, economical, and environmental aspects. There is also no drawback in terms of versatility and comonomer variation, and future studies will address the copolymerization of NDIBr$_2$ with other building blocks to yield highly efficient electron transport materials with yet improved performance.

■ ASSOCIATED CONTENT

ⓢ Supporting Information

Materials, methods, and additional characterization, including model compounds, assignments of chemical shifts, full NMR spectra, thermal characterization, additional UV−vis spectra, and additional FET characterization. The Supporting Information is available free of charge on the ACS Publications website at DOI: 10.1021/jacs.5b03355.

■ AUTHOR INFORMATION

Corresponding Authors
*komber@ipfdd.de
*michael.sommer@makro.uni-freiburg.de

Notes
The authors declare no competing financial interest.

■ ACKNOWLEDGMENTS

■ REFERENCES

(1) Anthony, J. E.; Facchetti, A.; Heeney, M.; Marder, S. R.; Zhan, X. *Adv. Mater.* **2010**, *22*, 3876.

(2) Zhan, X.; Facchetti, A.; Barlow, S.; Marks, T. J.; Ratner, M. A.; Wasielewski, M. R.; Marder, S. R. *Adv. Mater.* **2011**, *23*, 268.

(3) Schlitz, R. A.; Brunetti, F. G.; Glaudell, A. M.; Miller, P. L.; Brady, M. A.; Takacs, C. J.; Hawker, C. J.; Chabinyc, M. L. *Adv. Mater.* **2014**, *26*, 2825.

(4) Yan, H.; Chen, Z.; Zheng, Y.; Newman, C.; Quinn, J. R.; Dötz, F.; Kastler, M.; Facchetti, A. *Nature* **2009**, *457*, 679.

(5) Rivnay, J.; Toney, M. F.; Zheng, Y.; Kauvar, I. V.; Chen, Z.; Wagner, V.; Facchetti, A.; Salleo, A. *Adv. Mater.* **2010**, *22*, 4359.

(6) Caironi, M.; Bird, M.; Fazzi, D.; Chen, Z.; Di Pietro, R.; Newman, C.; Facchetti, A.; Sirringhaus, H. *Adv. Funct. Mater.* **2011**, *21*, 3371.

(7) Brinkmann, M.; Gonthier, E.; Bogen, S.; Tremel, K.; Ludwigs, S.; Hufnagel, M.; Sommer, M. *ACS Nano* **2012**, *6*, 10319.

(8) Sommer, M. *J. Mater. Chem. C* **2014**, *2*, 3088.

(9) Kim, R.; Amegadze, P. S. K.; Kang, I.; Yun, H.-J.; Noh, Y.-Y.; Kwon, S.-K.; Kim, Y.-H. *Adv. Funct. Mater.* **2013**, *23*, 5719.

(10) Luzio, A.; Fazzi, D.; Nübling, F.; Matsidik, R.; Straub, A.; Komber, H.; Giussani, E.; Watkins, S. E.; Barbatti, M.; Thiel, W.; Gann, E. H.; Thomsen, L.; McNeill, C. R.; Caironi, M.; Sommer, M. *Chem. Mater.* **2014**, *26*, 6033.

(11) Snoeij, N. J.; van Iersel, A. A.; Penninks, A. H.; Seinen, W. *Toxicol. Appl. Pharmacol.* **1985**, *81*, 274.

(12) Senkovskyy, V.; Tkachov, R.; Komber, H.; Sommer, M.; Heuken, M.; Voit, B.; Huck, W. T. S.; Kataev, V.; Petr, A.; Kiriy, A. *J. Am. Chem. Soc.* **2011**, *133*, 19966.

(13) Tkachov, R.; Karpov, Y.; Senkovskyy, V.; Raguzin, I.; Zessin, J.; Lederer, A.; Stamm, M.; Voit, B.; Beryozkina, T.; Bakulev, V.; Zhao, W.; Facchetti, A.; Kiriy, A. *Macromolecules* **2014**, *47*, 3845.

(14) Blouin, N.; Leclerc, M. *Acc. Chem. Res.* **2008**, *41*, 1110.

(15) Kowalski, S.; Allard, S.; Zilberberg, K.; Riedl, T.; Scherf, U. *Prog. Polym. Sci.* **2013**, *38*, 1805.

(16) Okamoto, K.; Zhang, J.; Housekeeper, J. B.; Marder, S. R.; Luscombe, C. K. *Macromolecules* **2013**, *46*, 8059.

(17) Facchetti, A.; Vaccaro, L.; Marrocchi, A. *Angew. Chem., Int. Ed.* **2012**, *51*, 3520.

(18) Wang, Q.; Takita, R.; Kikuzaki, Y.; Ozawa, F. *J. Am. Chem. Soc.* **2010**, *132*, 11420.

(19) Berrouard, P.; Najari, A.; Pron, A.; Gendron, D.; Morin, P.-O.; Pouliot, J.-R.; Veilleux, J.; Leclerc, M. *Angew. Chem.* **2012**, *124*, 2110.

(20) Lu, W.; Kuwabara, J.; Kanbara, T. *Macromolecules* **2011**, *44*, 1252.

(21) Morin, P.-O.; Bura, T.; Sun, B.; Gorelsky, S. I.; Li, Y.; Leclerc, M. *ACS Macro Lett.* **2015**, *4*, 21.

(22) Lu, W.; Kuwabara, J.; Iijima, T.; Higashimura, H.; Hayashi, H.; Kanbara, T. *Macromolecules* **2012**, *45*, 4128.

(23) Kowalski, S.; Allard, S.; Scherf, U. *ACS Macro Lett.* **2012**, *1*, 465.

(24) Chang, S.-W.; Waters, H.; Kettle, J.; Kuo, Z.-R.; Li, C.-H.; Yu, C.-Y.; Horie, M. *Macromol. Rapid Commun.* **2012**, *33*, 1927.

(25) Nohara, Y.; Kuwabara, J.; Yasuda, T.; Han, L.; Kanbara, T. *J. Polym. Sci., Polym. Chem.* **2014**, *52*, 1401.

(26) Lombeck, F.; Komber, H.; Gorelsky, S. I.; Sommer, M. *ACS Macro Lett.* **2014**, *3*, 819.

(27) Kowalski, S.; Allard, S.; Scherf, U. *Macromol. Rapid Commun.* **2014**, DOI: 10.1002/marc.201400557.

(28) Fujinami, Y.; Kuwabara, J.; Lu, W.; Hayashi, H.; Kanbara, T. *ACS Macro Lett.* **2012**, *1*, 67.

(29) Rudenko, A. E.; Thompson, B. C. *J. Polym. Sci., Polym. Chem.* **2015**, *53*, 135.

(30) Chen, Z.; Zheng, Y.; Yan, H.; Facchetti, A. *J. Am. Chem. Soc.* **2009**, *131*, 8.

(31) Guo, X.; Watson, M. D. *Org. Lett.* **2008**, *10*, 5333.

(32) Matsidik, R.; Martin, J.; Schmidt, S.; Obermayer, J.; Lombeck, F.; Nübling, F.; Komber, H.; Fazzi, D.; Sommer, M. *J. Org. Chem.* **2015**, *80*, 980.

(33) Steyrleuthner, R.; Schubert, M.; Howard, I.; Klaumünzer, B.; Schilling, K.; Chen, Z.; Saalfrank, P.; Laquai, F.; Facchetti, A.; Neher, D. *J. Am. Chem. Soc.* **2012**, *134*, 18303.

(34) Mercier, L. G.; Aïch, B. R.; Najari, A.; Beaupré, S.; Berrouard, P.; Pron, A.; Robitaille, A.; Tao, Y.; Leclerc, M. *Polym. Chem.* **2013**, *4*, 5252.

(35) Kohn, P.; Huettner, S.; Komber, H.; Senkovskyy, V.; Tkachov, R.; Kiriy, A.; Friend, R. H.; Steiner, U.; Huck, W. T. S.; Sommer, J.-U.; Sommer, M. *J. Am. Chem. Soc.* **2012**, *134*, 4790.

(36) Kohn, P.; Huettner, S.; Steiner, U.; Sommer, M. *ACS Macro Lett.* **2012**, *1*, 1170.

(37) Yuan, Y.; Giri, G.; Ayzner, A. L.; Zoombelt, A. P.; Mannsfeld, S. C. B.; Chen, J.; Nordlund, D.; Toney, M. F.; Huang, J.; Bao, Z. *Nat. Commun.* **2014**, *5*, 1.

(38) Sze, S. M.; Ng, K. K. *Physics of Semiconductor Devices*, 3rd ed.; John Wiley & Sons, Inc.: New York, 2006.

(39) Luzio, A.; Fazzi, D.; Natali, D.; Giussani, E.; Baeg, K.-J.; Chen, Z.; Noh, Y.-Y.; Facchetti, A.; Caironi, M. *Adv. Funct. Mater.* **2014**, *24*, 1151.

(40) Kim, N.-K.; Khim, D.; Xu, Y.; Lee, S.-H.; Kang, M.; Kim, J.; Facchetti, A.; Noh, Y.-Y.; Kim, D.-Y. *ACS Appl. Mater. Interfaces* **2014**, *6*, 9614.

(41) Chen, Z.; Lee, M. J.; Shahid Ashraf, R.; Gu, Y.; Albert-Seifried, S.; Meedom Nielsen, M.; Schroeder, B.; Anthopoulos, T. D.; Heeney, M.; McCulloch, I.; Sirringhaus, H. *Adv. Mater.* **2012**, *24*, 647.

(42) Lei, T.; Dou, J.-H.; Cao, X.-Y.; Wang, J.-Y.; Pei, J. *J. Am. Chem. Soc.* **2013**, *135*, 12168.

(43) Luzio, A.; Criante, L.; D'Innocenzo, V.; Caironi, M. *Sci. Rep.* **2013**, *3*, 3425.

(44) Park, J. H.; Jung, E. H.; Jung, J. W.; Jo, W. H. *Adv. Mater.* **2013**, *25*, 2583.

(45) Sun, B.; Hong, W.; Yan, Z.; Aziz, H.; Li, Y. *Adv. Mater.* **2014**, *26*, 2636.

(46) Kanimozhi, C.; Yaacobi-Gross, N.; Chou, K. W.; Amassian, A.; Anthopoulos, T. D.; Patil, S. *J. Am. Chem. Soc.* **2012**, *134*, 16532.

(47) Zhang, F.; Hu, Y.; Schuettfort, T.; Di, C.; Gao, X.; McNeill, C. R.; Thomsen, L.; Mannsfeld, S. C. B.; Yuan, W.; Sirringhaus, H.; Zhu, D. *J. Am. Chem. Soc.* **2013**, *135*, 2338.

(48) Estrada, L. A.; Deininger, J. J.; Kamenov, G. D.; Reynolds, J. R. *ACS Macro Lett.* **2013**, *2*, 869.

(49) Kuwabara, J.; Yasuda, T.; Choi, S. J.; Lu, W.; Yamazaki, K.; Kagaya, S.; Han, L.; Kanbara, T. *Adv. Funct. Mater.* **2014**, *24*, 3226.